DIRECT MEASUREMENT OF PLASTIC ZONES IN SIDE GROOVED FRACTURE TOUGHNESS SPECIMENS

S. Nunomura*, Y. Higo* and K. Seto**

INTRODUCTION

Plane strain fracture characteristics which are required in calculating unstable fracture resistance cannot be obtained unless an unstable fracture occurs in the testing procedure. To produce unstable fracture along the whole crack front in a specimen made of low or medium strength material, large size specimens and large capacity test equipment are required. It has been suggested, however, that completely catastrophic fracture is not necessary, and that it is sufficient to produce local fracture in the condition under consideration, provided that it is detected precisely [1]. Pop-in load measurements recommended in ASTM E399-74 are also in this category. The thickness requirement of $2.5(K_{IC}/\sigma_Y)^2$ seems to be a conservative value reflecting the present level of fracture detection techniques. When the techniques are improved, there are reports [1] [2] which show that the factor of the above requirement should be less than unity. Side grooved fracture toughness specimens are often employed and are regarded as improving the detectability of the local fracture. The technique is also used to keep the crack path straight in DCB specimens.

The effect of the side grooving is due to triaxial stresses, which restrict the strain in the thickness direction. Although many desirable effects of side grooving on plane strain fracture toughness tests have been reported, some still doubt the effect of side grooving on fracture detectability because the side groove increases triaxiality but reduces the net thickness of the specimen. Kanazawa analysed the triaxiality of side grooved Charpy impact bending specimens and showed that the degree of plane strain condition reduced with increased groove depth if the main crack was a fatigue crack and the side grooves were mechanical notches [3].

To prove the effect of side grooving, the stresses around the crack tip have to be examined. It is very hard to analyse even if the finite element method is used, because it is a three dimensional problem. In the work reported in this paper, the authors have measured directly the plastic zone configurations around the crack tip of side grooved fracture toughness specimens.

EXPERIMENTAL PROCEDURE

Hardness distribution, dislocation (etch pit) distribution and slip mark observation were used for the plastic zone observation. Observations of surface structure and the distortion of grids previously marked on the surface were also used to detect the plastic zone on the free surface of

*Research Laboratory of Precision Machinery and Electronics, Tokyo Institute of Technology, Tokyo, Japan.
**Tateyma Aluminum Work KK., Toyama, Japan.

the specimen, but these two could not be applied to the three dimensional problem. In using the three above mentioned methods, it is hard to avoid the effects of plastic flow which occurs during specimen cutting and grinding. Only the profiles of the plastic zone where the strain was greater than 5% were detectable. Here only the stress distribution around the crack tip was required, not the strain distribution.

The authors used a stress assisted martensitic transformation to observe the plastic zone configuration. The fracture toughness specimen (Figure 1) was made of an 18-8 type austenitic stainless steel, whose Md temperature was below room temperature. After the main notch had been sharpened with a low stress fatigue crack, side grooves were cut by an electric discharge machine using a flat electrode formed by rolling fine wire whose diameter was 0.08mm. The specimen was then heat-treated by vacuum to obtain the desirable Ms temperature. The bend test was performed in an Instron type testing machine with a fitted specimen cage. At a fixed load, the cage was submersed in coolant which was kept at a temperature between the Md and Ms points of the material. At this temperature, the martensitic transformation should occur in grains where the resolved shear stress on any slip plane exceeds the shear yield strength at that temperature. This partially transformed specimen was cut into pieces along the x-y and x-z planes (Figure 1) by the electric discharge machine. The cut surfaces were mechanically polished through 800 grit metallographic paper and electrochemically polished and etched in a solution of 90 parts CH_3COOH and 10 parts 60% H_2O_2.

All over the polished surfaces, low magnitude micro-photographs were taken. Two depths of side groove, 1mm and 2mm, were used, and designated G1 and G2 side grooved specimens respectively. Their side groove ratios (t_g/t_n) were 1.25 and 1.67, where t_g and t_n were the gross and net thickness of the side grooved specimen respectively.

RESULTS AND DISCUSSION

The configuration of the plastic zone in a plain specimen which was tested to compare with the side grooved one had the well known hand-drum shape, but its detailed dimensions did not agree either with those from Irwin's simple formulae or with those from more accurate analyses by Tuba [4] or Rice and Rosengren [5]. To discuss the effect of side grooving, it seems to be important to compare the degrees of disturbance of the plane strain condition on the x-z plane at y = 0. The plain specimen for comparison is called the G0 specimen hereafter. The whole configuration of the plastic zone around the crack tip of a plain specimen will be discussed in another paper.

The stress intensity factor for the plain specimen was determined using the 3 point beam stress intensity factor solution and it was about 42 MPa.$m^{1/2}$ for G0 specimens. Optical micro-photographs of magnitude x80 mag. on the x-z plane were glaced in a montage in accordance with their co-ordinates (Photo. 1a).

The assembled photographs were carefully inspected to find the α-martensitic transformed grains. Transformed martensite was deposited on the slip planes, so that the martensitic transformed grain was easy to distinguish from untransformed grains. Photo. 2 shows clearly transformed grains in a side grooved specimen. A survey map of the cut surface of a plain specimen is given in Figure 2, where the open circles

mark the position of the transformed grains furthest from the crack in the x-direction. The solid line connecting the open circles shows the outer boundary of the transformed region, i.e. it could be regarded as the elastic/plastic boundary. As the fatigue crack front was not straight and had a tendency to tunnel, the elastic/plastic boundary under plane strain conditions was a curve parallel to the crack front.

At y = 0, the plastic zone size in the x-direction was given by the following equations in plane strain:

$$\gamma_{Ix} = \frac{1}{6\pi}\left(\frac{K}{\sigma_y}\right)^2 \tag{1a}$$

or for plane stress:

$$\gamma_{x} = \frac{1}{\pi}\left(\frac{K}{\sigma_y}\right)^2 \tag{1b}$$

Substituting K = 42.1 MPa.$m^{1/2}$ and σ_y = 218 MPa in these equations gives the values of γ_{Ix} and γ_x as 2.1mm and 12.6mm repsectively. The average plane strain plastic zone size was 2.0mm (Figure 2), which agrees closely with that given by equation (1a). The plane stress plastic zone size calculated was more than twice that observed on free surfaces. It was about 5mm in Figure 2. The reason for this difference seems to be that only a very thin layer near the surfaces is in plane stress and all grains at the free surfaces were larger than the thickness of this layer, so that they could not transform in accordance with the calculated stress distribution.

The side grooved specimens which had been loaded at the prescribed temperature were sectioned on the plane including the crack front and the bottom lines of the side grooves. These cut planes were treated in similar manner to the plain specimen. Photo. 1b shows the assembled micrographs for G2 side grooved specimens, and it consists of 126 separate micrographs. Examples of the plastic zone profiles on the x-z plane at y = 0 of G1 and G2 specimens are given in Figure 3 and Figure 4 respectively.

The stress intensity factor for the side grooved specimen is given by the following expression [6]:

$$K = K^*\left(t_g/t_n\right)^m \tag{2}$$

where K* is the stress intensity factor for a plain specimen whose thickness is t_g. The exponent m is a constant and is 0.5 theoretically, but it is found experimentally to be a material constant ranging between 0.5 and 1.0. To give the same stress intensity in the grooved specimens as in the G0 specimen, the loads for G1 and G2 specimens were calculated using equation (2) and taking the exponent m to be 0.5. The plastic zone sizes of G1 and G2 side grooved specimens shown in Figure 3 and Figure 4 were 2.5mm and 2.4mm respectively. The difference in the plastic zone sizes of the side grooved specimens compared with the plain specimen seems to arise in the stress intensity factor calculation, i.e. taking an incorrect value of the exponent m in equation (2). The value of m obtained by the reverse calculation was about 0.7, with a wide scatter. Plane stress plastic zone size could not be obtained because no plane stress regions existed at the bottom of the side grooves.

The angle between the elastic/plastic boundary and the specimen surface at y = 0 was almost $\pi/4$ according to observations for many G0 specimens. Although the solid line did not pass through the open circle just under the surface in Figure 2, it was due to no grain with preferred orientation there. Since one of the maximum shear stress directions made an angle of $\pi/4$ to the surface, the authors had considered at first that the oblique line intersected the surface at the elastic/plastic boundary of the plane stress region [1]. However, the oblique line intersected at a point located closer to the crack than estimated and it was convenient for the small scale fracture test. The angle of the oblique line to the x-axis may be smaller than that in the plain specimen.

At the moment the stress intensity in the plane strain region in the mid-section of a thick specimen reaches K_{IC}, fracture should start there. In the surrounding non-plane strain region, however, the fracture has not occurred at this stress intensity factor so that the crack at the mid-section may not continue to propagate and may arrest due to the restraint of the unfractured zone. Then the valid plane strain fracture characteristic can be determined if there is a plane strain region and the initiation of local fracture can be detected. Therefore the ratio of the plane strain region to the non-plane strain region affects the detectability.

As a qualitative evaluation, the ratios of (area of hatched zone) to (area of plastic zone except hatched zone) were calculated from Figure 2, Figure 3 and Figure 4. The ratios for G0, G1 and G2 specimens were 27%, 15% and 8% respectively. These values indicated that the detectability of the local fracture improved with increasing the side groove depth. However, there should be an optimum side groove depth because the plane strain fracture characteristic is obtained only when the fracture occurs under plane strain conditions. The boundary intersects the surface at an angle, even in the side grooved specimen, and the plane strain region decreases with increasing stress intensity factor and/or decreasing the net thickness. Therefore it was impossible to obtain the K_{IC} of this material at any side groove depth with the specimen in Figure 1.

CONCLUSION

Plastic zones around the crack tip of the side grooved fracture toughness specimen were directly observed using a new technique applying the stress assisted martensitic transformation. Since the austenite phase transforms to the α-martensite phase only at loading temperature in this technique, the effect of plastic flow caused by specimen preparation at room temperature is negligible. The advance of this technique is also based upon the stress assisted transformation, but not strain induced phenomenon.

It was observed that the non-plane strain region at the extension of the notch plane was restricted by the side groove due to the triaxiality. The effect of the side grooving on the measurement of plane strain fracture characteristics using small specimens was demonstrated. The optimum depth of side groove and the limitations in its use were discussed.

REFERENCES

1. NUNOMURA, S., Bul. Tokyo Inst. of Tech., 131, 1975, 45.
2. MAY, M. J., ASTM STP436, 1970, 42.
3. KANAZAWA, T., J. Japan Soc. Ship Build., 91, 1952, 55.

4. TUBA, I. S., J. Strain Analysis, 1, 1966, 115.
5. RICE, J. R. and ROSENGREN, G. F., J. Mech. Phys. Sol., 16, 1968, 1.
6. NUNOMURA, S. and TANAKA, M., Proc. ICM Kyoto, 1, 1972, 485.

Photograph 1 Assembled Microphotographs of x-z Plane at y = 0. Crack Front and Elastic/Plastic Boundary Could be Observed.

(a) G0 Plain Specimen
(b) G2 Side Grooved Specimen

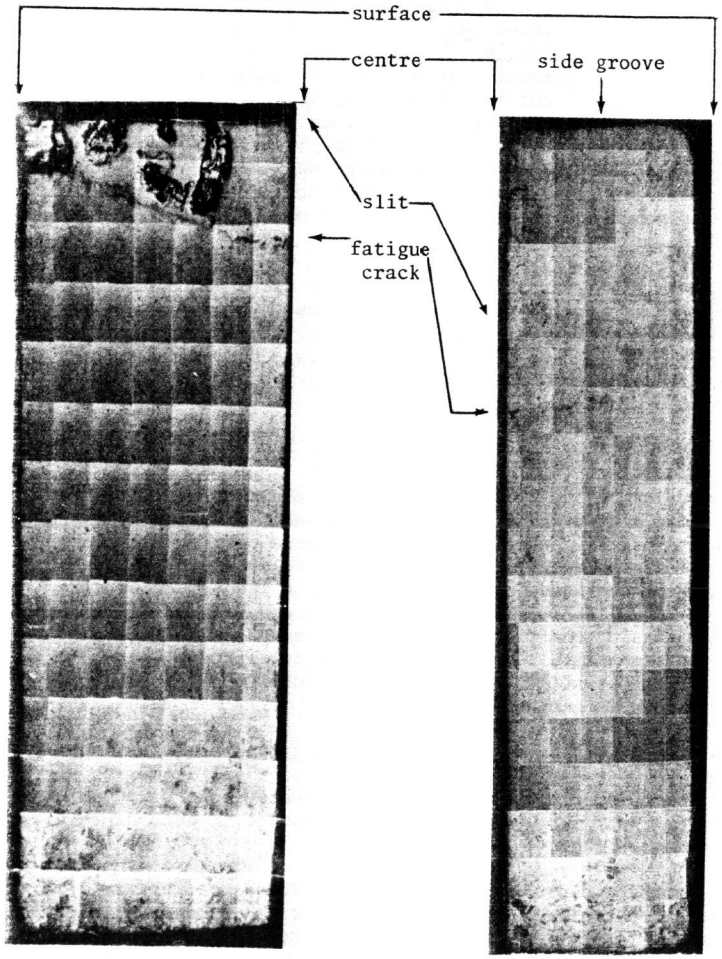

(a) (b)

Photograph 2 Martensitic Transformed Grains (Circles) Near the Bottom of Side Groove. α-Martensite Deposited on Slip Band

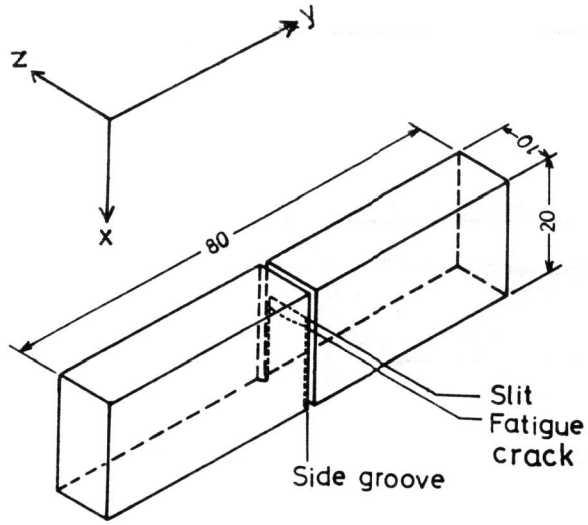

Figure 1 Shape and Size of Side Grooved Notched Bend Specimen. Cutting Plane Used to be Indicated with the Co-ordinates in this Figure where Mechanical Slit was on y = 0

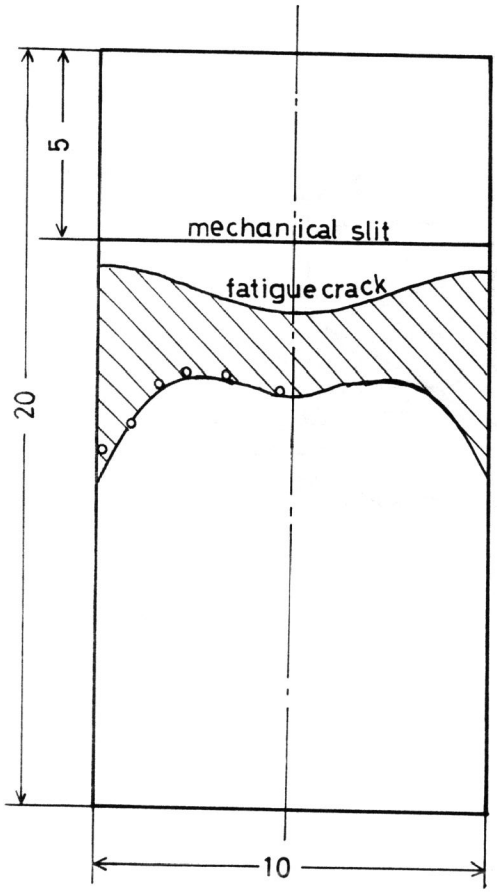

(2)

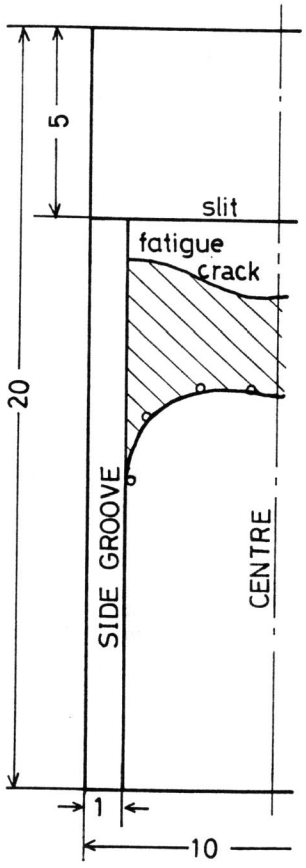

(3)

Figure 2 and 3 Survey Maps of the Plastic Zone Around the Crack Tip. These were Plotted Based on the Assembled Microphotographs for a GO Plain Specimen (Figure 2), and for G1 Side Grooved Specimen (Figure 3)

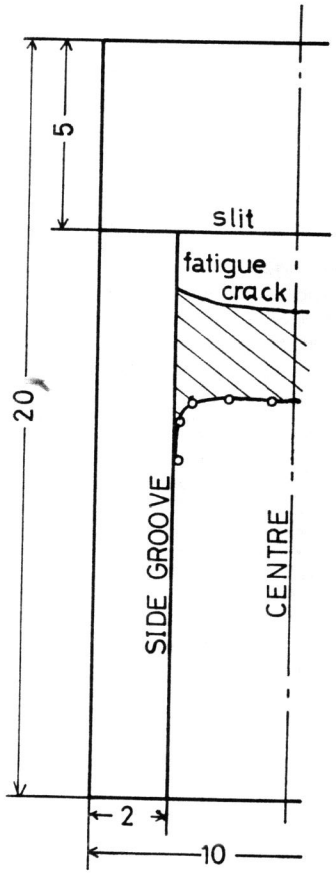

Figure 4 Survey Map of the Plastic Zone Around the Crack Tip. This was Plotted Based on the Assembled Microphotograph for a G2 Side Grooved Specimen

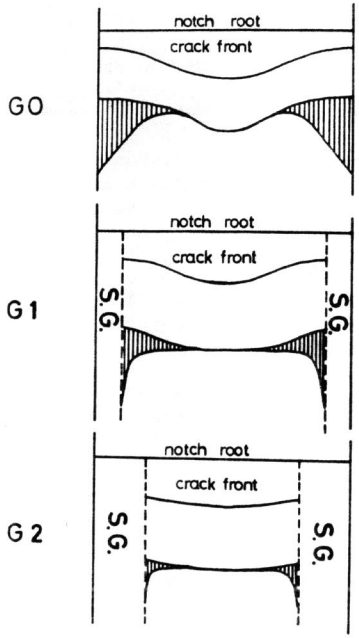

Figure 5 Effects of the Side Groove on Restriction on the Disturbance of Plane Strain Condition. Hatched Area Represented the Degree of the Disturbance